Analyzing Pedestrian Behavior in Crowds for Automatic Detection of Congestions

Barbara Krausz, Christian Bauckhage
Fraunhofer IAIS
53754 Sankt Augustin, Germany
{barbara.krausz, christian.bauckhage}@iais.fraunhofer.de

Abstract

Congestions in pedestrian traffic typically occur when the number of pedestrians exceeds the capacity of pedestrian facilities. In some cases, the pedestrian density reaches a critical level which may lead to a crowd stampede as happens rather frequently at mass gatherings, in stadiums or at train stations.

In the past, research has focused on improving simulations of crowd motion in order to identify potentially dangerous locations and to direct pedestrian streams. Recently, works towards the automatic real-time detection of critical mass behavior based on optical flow computations have been proposed. In this paper, we verify these approaches by analyzing mircoscopic pedestrian behavior in congestions and conducting experiments on synthetic as well as on real datasets.

1. Introduction

Congestions of vehicles have been studied intensively over the years [4]. In contrast to vehicular traffic, congestions in pedestrian traffic are not only annoying, but might become very dangerous. For example, when buildings have to be evacuated, people might be trapped in a congestion and cannot escape from the building early enough. In other cases, the number of pedestrians exceeds the capacity of pedestrian facilities which might even lead to stampedes as happend at the Loveparade 2010 in Duisburg, Germany, see Figure 1. During that event, 21 people died and more than 500 people were injured, since some parts of the festival area were too small to accommodate thousands of visitors.

In order to avoid such hazardous situations, simulations are conducted for directing pedestrian streams and defuse locations that are potentially dangerous. Here, insights into pedestrian behavior help to improve and validate simulations of pedestrian streams and to optimize locations and dimensions of emergency exits when developing evacuation strategies.

Figure 1. Congestion at the Loveparade 2010 in Duisburg, Germany [15].

However, the Loveparade disaster and other deadly stampedes show that crowds of people might become unmanagable and unpredictable. Recently, works towards the real-time detection of congestions in pedestrian traffic have been proposed [11, 12]. These works compute optical flow features and detect critical motion behavior in crowds. In this paper, we confirm this approch by analyzing microscopic characteristics of human motion behavior in congested areas and test visual features proposed in [11, 12] on a synthetic dataset as well as on videos recorded at the Loveparade 2010.

2. Related work

Pedestrian dynamics have been studied intensively for more than 40 years. Recently, knowledge about crowd dynamics has been used to improve evacuation strategies in emergency situations and to prevent congestions and overcrowding. Here, simulations are a standard tool in the study of large groups of pedestrians. Physical models modeling pedestrians based on the analogy to gases, fluids or granulates have been developed in order to account for individual behavior. The *social force model* [8, 6] as well as *cellular*

automata [3, 10] which both model pedestrian dynamics on a microscopic level are among the more widely used approaches.

In order to improve and validate models of pedestrian behavior, insights into human motion characteristics are needed. Especially, the dynamics in locations of high pedestrian density are of great interest, since pedestrian simulations are used in order to develop evacuation strategies. Researchers conduct different experiments for analyzing human motion at bottlenecks on a macroscopic as well as on a microscopic level. In particular, Hoogendoorn and Daamen [9] examine human walking characteristics and phenomena like lane formation at bottlenecks. Kretz et al. [13] relate parameters such as evacuation times and flow to the width of the bottleneck. Similar to that, Seyfried and Schadschneider [24] analyze the relationship between the dimensions of the bottleneck and the density and pedestrian flow. The most comprehensive study can be found in [5]. Here, Daamen and Hoogendoorn analyze the influence of various parameters like age, number of disabled people, illumination conditions and stress level.

Works related to real-time analysis of human crowds can be found in the computer vision community. In the last years, ideas adopted from simulations of pedestrian dynamics were incorporated into the design of visual tracking systems [2, 16]. More recently, works towards real-time detection of hazardous situations in human crowds have been proposed by Krausz and Bauckhage [11, 12]. They make use of characeristic motion patterns in congestions and propose optical flow features for congestion detection.

3. The Fundamental Diagram

According to Schadschneider et al. [21], congestions occur in locations of high density where the inflow exceeds its capacity. These locations are called bottlenecks and have been studied for example in [9, 24, 5]. Besides bottlenecks, jamming can also be observed in locations where two opposing pedestrian streams clash resulting in high densities and low velocities.

In pedestrian dynamics, this relationship between density ρ and velocity v is captured by the *fundamental diagram*. The most frequently cited version is the fundamental diagram given by Weidmann [27] who evaluated 25 different datasets. Basically, the fundamental diagram shows decreasing velocities for increasing densities, although diagrams found by others [20, 17, 7] differ from the graph shown in Figure 2.

Seyfried et al. [25] sub-divide the range of densities into four different domains each having a different decrease of velocity. Essentially, the domains III ($2.3 \leq \rho \leq 4.7$) and IV ($\rho \geq 4.7$) (see Figure 2) correspond to congestions where physical contact between pedestrians is hardly avoidable. Here, the velocity has dropped to a low level (< 0.5 m/s), whereas Weidmann [27] gives an average velocity of 1.34 m/s for normal walking conditions.

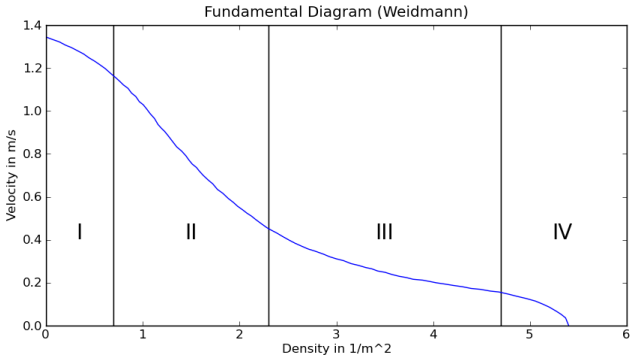

Figure 2. Fundamental diagram according to Weidmann [27] measuring the relationship between density ρ and velocity v. The diagram is based on 25 different datasets. The range of densities is sub-divided into four domains of different decrease of velocities where domains III and IV correspond to congestions, see [25].

In their later work [23], Seyfried et al. investigate the relationship between density and velocity on a microscopic level by tracking single pedestrians and measuring microscopic motion characteristics based on obtained trajectories [26]. Observing the probability distribution of velocities for fixed densities, they find two peaks for high densities reflecting the two phases of *stop-and-go waves*. Stop-and-go waves show alternating forward pedestrian motion and backward gap propagation and have been observed by researchers in locations of high pedestrian density where an unobstructed pedestrian flow becomes impossible [7, 19, 18]. Seyfried et al. give a density of $2.2m^{-1}$ above which a moving and a stopping phase can be observed.

4. Pedestrian Behavior in Congested Areas

On a microscopic level, pedestrian behavior at various velocities give valuable insights into human behavior in congested areas. We analyze trajectories obtained from video recordings of a large scale experiment conducted under laboratory conditions [1, 22]. Pedestrian groups of varying sizes ($N = 14, 17, \ldots, 62, 70$) walk through a corridor recorded by topview cameras.

As expected, we first observe that the mean velocity of the pedestrians decreases for increasing group sizes. Second, from the trajectories, we can observe that people do not move along a straight line, instead, it is a characteristic of human gait, that humans tend to swing laterally. Furthermore, comparing trajectories of pedestrians walking at different speeds reveals substantial differences. One can clearly see differences both in the frequency and the amplitude of lateral swaying. Similar findings have been reported by Hoogendoorn and Daamen [9] and Liu et al. [14].

Figure 3 shows the relationship between velocities and

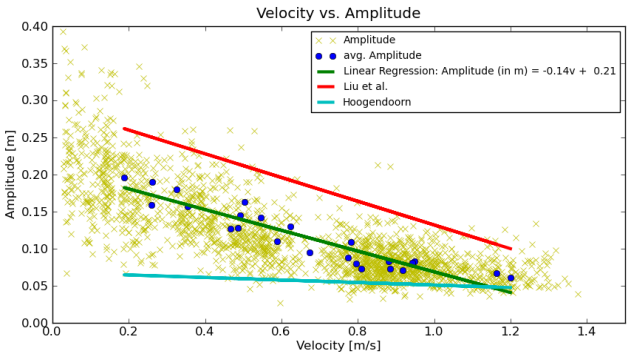

Figure 3. Relationship between velocitiy and amplitude of lateral oscillation in comparison to the findings of Liu et al. [14] as well as Hoogendoorn and Daamen [9]. Blue markers correspond to mean velocity and mean amplitude of different pedestrian groups.

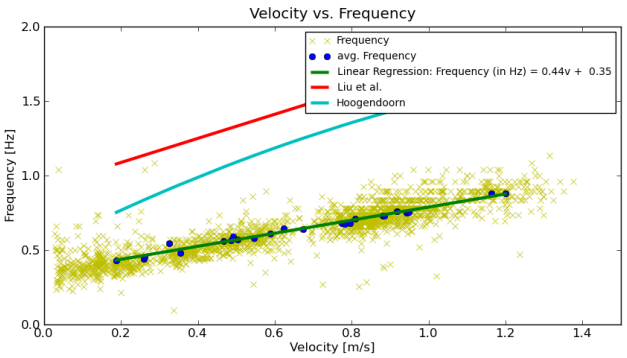

Figure 4. Relationship between velocitiy and frequency of lateral oscillation in comparison to the findings of Liu et al. [14] as well as Hoogendoorn and Daamen [9]. Blue markers correspond to mean velocity and mean frequency of different pedestrian groups.

amplitudes of lateral oscillation. We find amplitudes in the range between 6 cm and approx. 30 cm. Fitting a linear model, we find a negative relationship between the amplitude a (in m) and the velocity v (in m/s):

$$a = -0.14v + 0.21 \tag{1}$$

which is comparable to the findings of Liu et al. [14] as well as Hoogendoorn and Daamen [9]. We argue that humans tend to swing laterally when walking slowly in order to keep their balance.

Next, we analyze the frequency of lateral oscillations which is depicted in Figure 4. Similar to amplitudes, we find a linear relationship between frequencies and velocities, but, in contrast, frequencies increase with increasing velocities. By fitting a linear model, we find that the frequency f (in Hz) is related to the velocity v (in m/s) as follows:

$$f = 0.44v + 0.35. \tag{2}$$

Although Liu et al. also find a linear relationship, the frequencies observed in their experiments are higher than in our experiments. Hoogendoorn and Daamen fit a quadratic function which is in accordance to the results reported in [14], see Figure 4.

Having analyzed space requirements in lateral direction, we also analyze space requirements in longitudinal direction. Figure 5 depicts the relationship between velocity v (in m/s) and the distance d (in m) to the pedestrian in front. Similar to Seyfried et al. [25], we find a linear relationship between those quantities:

$$d = 1.5v + 0.0035. \tag{3}$$

Summarizing, we find that the amplitude of lateral oscillation is high for people walking slowly in a congested area whereas the frequency of that oscillation is smaller compared to walking with normal speed. Finally, the distance to the pedestrian in front tends to be smaller when walking slowly in a congestion.

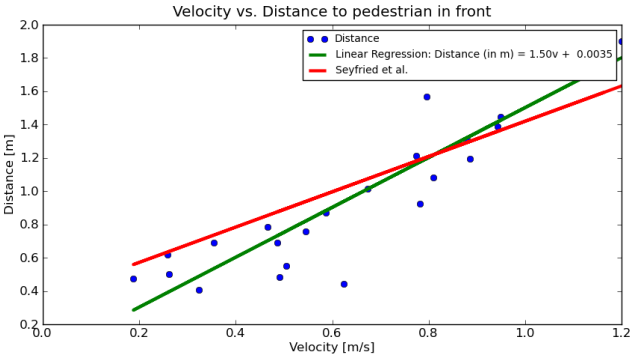

Figure 5. Relationship between mean velocitiy and mean distance to the pedestrian in front in comparison to the findings of Seyfried et al. [25].

5. Features for Congestion Detection

Due to the huge number of people at mass gatherings, occlusions as well as privacy concerns, traditional tracking approaches are often not feasible and, hence, direct measurements of velocities are not possible. Instead, in [11, 12], Krausz and Bauckhage propose to make use of the observation that the amplitude of lateral oscillation increases for low velocities in order to detect congestions. They compute dense optical flow fields where two subsequent frames are compared in order to determine motion direction and magnitude for each pixel. Next, they compute two-dimensional histograms of motion direction and magnitude of all flow vectors. Then, histograms are averaged over a short time interval. Histograms that are indicative of congestion situations show motion along two major directions (rightwards and leftwards) which reflect lateral oscillation of the people's upper bodies. Such histograms show a high degree of symmetry (see Figure 6) so that the mirror symmetry of an optical flow histogram is measured and considered a feature for congestion detection.

They compute the symmetry measure by summing

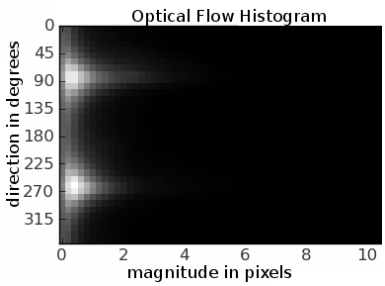

Figure 6. A 2D – histogram of motion direction and magnitude of optical flow vectors. This histogram is characteristic for motion in congestion situations. Mainly, it shows small motion along two major directions. This left- and rightward motion is caused by people swinging laterally to keep their balance.

the absolute differences between the 2D-histogram and a flipped version of itself. In order to account for effects of viewing perspective, each frame is subdivided into a set of cells with cells in the background of the scene being smaller. Let $H_{i,c}(dir, mag)$ be the two-dimensional histogram of direction and magnitude of cell c at time i. Then, flipping $H_{i,c}(dir, mag)$ around a horizontal symmetry axis at 180° and denoting it by $\hat{H}_{i,c}(dir, mag)$, the value is computed as

$$sym_{i,c} = \sum_{dir,mag} w(dir) \cdot \left| \hat{H}_{i,c}(dir, mag) - H_{i,c}(dir, mag) \right|. \tag{4}$$

We set $sym_{i,c} = 0$, if no apparent motion is visible, i.e. if $\sum_{dir} H_{i,c}(dir, 0) > 0.98$. We extend the original feature [11, 12] by introducing a weight $w(dir)$ computed as:

$$w(dir) = \begin{cases} \frac{|dir - 90°|}{10°} & dir \leq 180° \\ \frac{|dir - 270°|}{10°} & dir > 180° \end{cases} \tag{5}$$

The weight for 90° and 270° is 0 whereas it has its maximum value of 9 for 0°, 180° and 360°. Accordingly, low values of $sym_{i,c}$ indicate that $H_{i,c}(dir, mag)$ is highly mirror-symmetric with peaks around 90° and 270° and is indicative for a congestion.

6. Experiments

It was stated above, that low values $sym_{i,c}$ indicate a congested area. However, the scale of this quantity depends on different factors, such as the camera view point, the number of people visible in the scene as well as the environment. In order to overcome this problem, Krausz and Bauckhage [11, 12] learn typical values of $sym_{t,c}$ and detect deviations for identifying anomalies and congestions by applying a sequential change-point detection algorithm. Here, it is of vital importance that phases of different pedestrian flow result in different values of the feature described in section 5. In

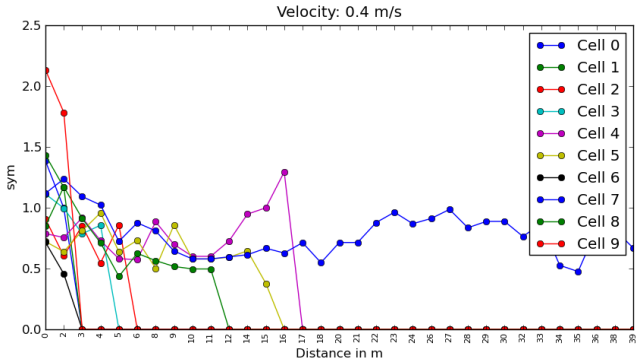

Figure 7. Relationship between feature values and distance to the camera for an artificial video sequence with a single pedestrian walking with a velocity of 0.4 m/s on an ideal trajectory towards the camera. One can observe that $sym_{i,c}$ increases to a value > 0 for different cells c as the pedestrian crosses cell c. Note that $sym_{i,c} = 0$, if no motion is observed in cell c at timepoint i.

the following, we verify this assumption by applying this feature to synthetic datasets as well as to the Loveparade dataset.

6.1. Synthetic Dataset

In our first experiment, we use the linear relationships (equations 1 to 3) that we found by analyzing the trajectories obtained from the large scale experiment (section 4) and generate artificial videos of a pedestrian walking with different speeds ($v = 0.2, 0.4, \ldots, 1.2, 1.4$) on an ideal trajectory towards the camera.

We subdivide the frame into a grid of cells and compute the feature described in section 5 based on optical flow histograms averaged over different time intervals. Figure 7 shows the development of $sym_{i,c}$ depending on the distance of the pedestrian to the camera. The value of $sym_{i,c}$ increases for a cell c, when the pedestrian crosses c. Interestingly, the time offset of the curves for different cells is clearly visible.

Primarily, we are interested in the difference between the feature values for different velocities. Figure 8 shows mean feature values over all cells for a single pedestrian as well as for a group of 50 pedestrians walking with different velocities. Obviously, the feature value is lower for lower velocities. In addition to that, we vary the time interval for averaging optical flow histograms (25, 50 and 75 frames).

From Figure 8, we can observe that the difference between normal velocities and velocities ≤ 0.6 m/s observable in congestions is increased when more pedestrians are visible. This comes from the fact that more left and right movements are performed when multiple pedestrians are walking. Furthermore, Figure 8 reveals no significant differences between different time intervals for averaging optical flow histograms.

In the next experiment, we focus on phase changes. We

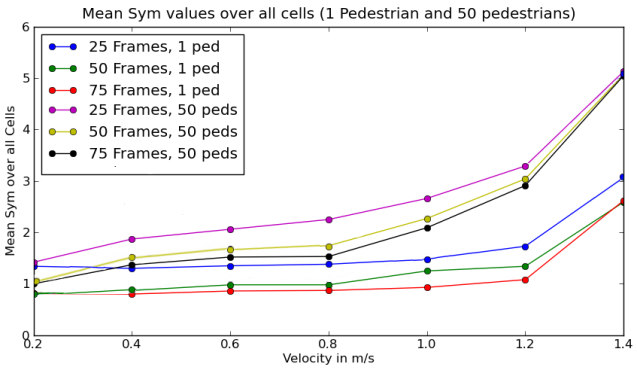

Figure 8. Mean feature values over all cells for a single pedestrian as well as for a group of 50 pedestrians walking with different velocities.

generated synthetic videos of 50 people walking fast and then abruptly decrease their speed. Again, we compute $sym_{i,c}$ for all cells c and sum up all values giving sym_i. Then, we compute the mean and the standard deviation of sym_i for the phase with high velocity, denoted as μ_1 and σ_1, as well as the mean of sym_i for the second phase of low velocities, denoted as μ_2. Now, we check if the values in the first phase differ significantly from values in the second phase by checking if $|\mu_1 - \mu_2| > 2 \cdot \sigma_1$. Table 1 gives results for different configurations. It shows that phases of different velocities are mapped to different ranges of feature values for most of the tested configurations. Importantly, the feature can distinguish between velocities observed in normal walking conditions (average walking speed 1.34 m/s [27]) and velocities typically observed in congestions ($\leq$ 0.6 m/s). Moreover, we do not observe any difference between different time intervals for averaging optical flow histograms.

6.2. Loveparade Dataset

We tested the feature presented in section 5 on video footage from the crowd disaster at the Loveparade 2010 in Duisburg [15]. Figure 9 shows phases of different pedestrian flow that are well reproduced by the proposed feature. To create this plot, we averaged histograms of optical flow over a time period of 10 seconds and summed the values of $sym_{i,c}$ for the cells in the scene foreground. From the graph, one can identify unusual events and, notably, the congestion is characterized by feature values at a very low level. By applying a sequential change-point detection algorithm [11, 12], these unusual events and congestions can be detected automatically.

7. Conclusions

Congestions in pedestrian traffic may lead to over-critical densities of pedestrians. Knowledge about pedestrian behavior in crowds not only helps to improve simulations. It is also incorporated into methods for automatic detection of hazardous sitations. We verified such approaches by analyzing trajectories obtained from a large scale experiment and discuss visual features based on optical flow computations which detect characteristic human motion patterns in congested areas. We conducted various experiments on synthetic as well as on real datasets in order to show its effectiveness.

Phases $v_1 \Rightarrow v_2$	25 Frames	50 Frames	75 Frames
1.4 m/s $\Rightarrow$ 0.6 m/s	✓	✓	✓
1.4 m/s $\Rightarrow$ 0.4 m/s	✓	✓	✓
1.4 m/s $\Rightarrow$ 0.2 m/s	✓	✓	✓
1.2 m/s $\Rightarrow$ 0.6 m/s	✓	✓	✓
1.2 m/s $\Rightarrow$ 0.4 m/s	✓	✓	✓
1.2 m/s $\Rightarrow$ 0.2 m/s	✓	✓	✓
1.0 m/s $\Rightarrow$ 0.6 m/s	✓	✓	✓
1.0 m/s $\Rightarrow$ 0.4 m/s	✓	✓	✓
1.0 m/s $\Rightarrow$ 0.2 m/s	✓	✓	✓
0.8 m/s $\Rightarrow$ 0.6 m/s	-	-	-
0.8 m/s $\Rightarrow$ 0.4 m/s	-	-	-
0.8 m/s $\Rightarrow$ 0.2 m/s	-	✓	✓

Table 1. Results obtained from artificial videos with two phases. In the first phase, pedestrians walk with velocity v_1 and decrease their velocity to v_2 in the second phase. We check if the values in the first phase differ significantly from the values of the second phase, i.e. if $|\mu_1 - \mu_2| > 2 \cdot \sigma_1$. Moreover, we vary the time interval for averaging optical flow histograms from 25 frames to 75 frames.

References

[1] DFG Research Project. http://www2.fz-juelich.de/jsc/appliedmath/ped/projects/dfg, 2011. 2

[2] S. Ali and M. Shah. Floor fields for tracking in high density crowd scenes. In *ECCV*, 2008. 2

[3] C. Burstedde, K. Klauck, A. Schadschneider, and J. Zittartz. Simulation of pedestrian dynamics using a 2-dimensional cellular automaton. *Physica A*, 295(3–4):507–525, 2001. 2

[4] D. Chowdhury, L. Santen, and A. Schadschneider. Statistical physics of vehicular traffic and some related systems. *Physics Reports*, 329(4–6):199–329, 2000. 1

[5] W. Daamen and S. Hoogendoorn. Capacity of doors during evacuation conditions. *Procedia Engineering*, 3:53 – 66, 2010. 2

[6] D. Helbing, I. Farkas, and T. Vicsek. Simulating dynamical features of escape panic. *Nature*, 407(6803):487–490, 2000. 1

[7] D. Helbing, A. Johansson, and H. Z. Al-Abideen. Dynamics of crowd disasters: An empirical study. *Physical Review E*, 75(4):046109–1–7, 2007. 2

[8] D. Helbing and P. Molnár. Social force model for pedestrian dynamics. *Physical Review E*, 51(5):4282–4286, 1995. 1

[9] S. P. Hoogendoorn and W. Daamen. Pedestrian behavior at bottlenecks. *Transp. Science*, 39:147–159, 2005. 2, 3

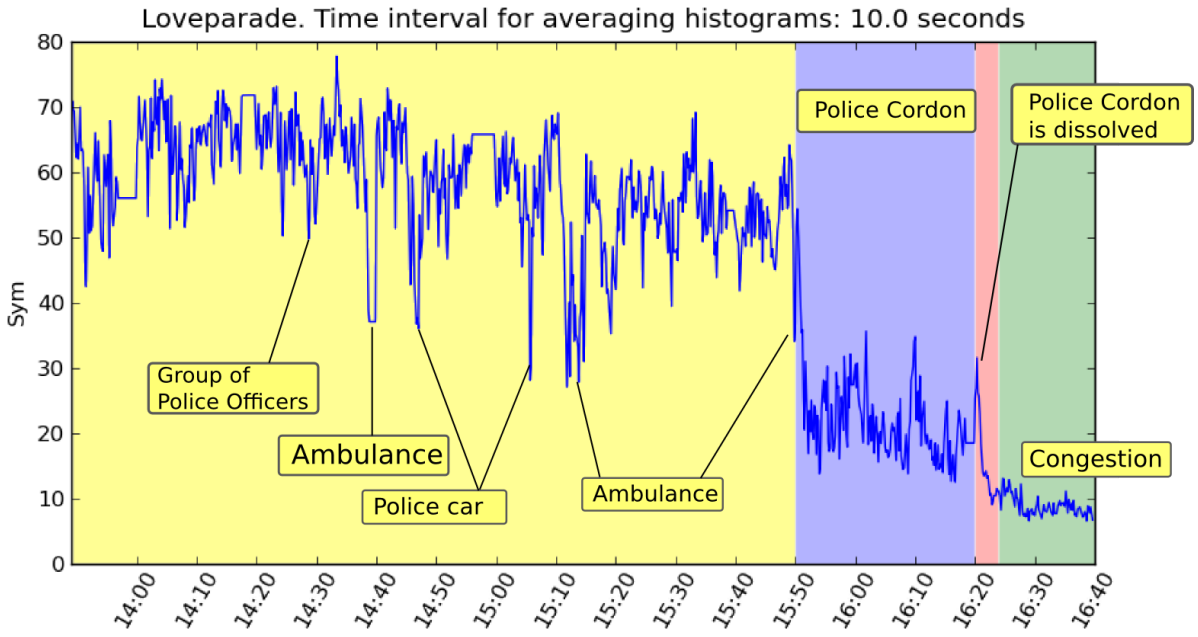

Figure 9. Development of $sym_{i,c}$ measuring the mirror symmetry of the optical flow histograms. One can clearly distinguish phases of different pedestrian flow as well as unusual events such as police cars crossing the scene. In particular, the congestion is characterized by extremly low values of $sym_{i,c}$. By applying a sequential change-point detection algorithm [11, 12], unusual events and congestions can be detected automatically.

[10] A. Kirchner and A. Schadschneider. Simulation of evacuation processes using a bionics-inspired cellular automaton model for pedestrian dynamics. *Physica A*, 312(1-2):260–276, 2002. 2

[11] B. Krausz and C. Bauckhage. Automatic detection of dangerous motion behavior in human crowds. In *AVSS*, 2011. 1, 2, 3, 4, 5, 6

[12] B. Krausz and C. Bauckhage. Loveparade 2010: Automatic video analysis of a crowd disaster. *CVIU (to appear)*, 2011. 1, 2, 3, 4, 5, 6

[13] T. Kretz, A. Grunebohm, and M. Schreckenberg. Experimental study of pedestrian flow through a bottleneck. *Journal of Statistical Mechanics*, 2006. 2

[14] X. Liu, W. Song, and J. Zhang. Extraction and quantitative analysis of microscopic evacuation characteristics based on digital image processing. *Physica A*, 388(13):2717–2726, 2009. 2, 3

[15] Lopavent. Dokumentation Loveparade. www.dokumentation-loveparade.com, 2010. 1, 5

[16] R. Mehran, A. Oyama, and M. Shah. Abnormal crowd behavior detection using social force model. In *CVPR*, 2009. 2

[17] M. Mori and H. Tsukaguchi. A new method for evaluation of level of service in pedestrian facilities. *Transp. Res.-A*, 21(3):223–234, 1987. 2

[18] A. Portz and A. Seyfried. Analyzing stop-and-go waves by experiment and modeling. In *Pedestrian and Evacuation Dynamics*, 2010. 2

[19] A. Portz and A. Seyfried. Modeling stop-and-go waves in pedestrian dynamics. In *Parallel Processing and Applied Mathematics*, 2010. 2

[20] V. M. Predtechenskii and A. I. Milinskii. Planning for foot traffic flow in buildings. *Amerind Publishing*, 1969. 2

[21] A. Schadschneider, W. Klingsch, H. Klüpfel, T. Kretz, C. Rogsch, and A. Seyfried. Evacuation dynamics: Empirical results, modeling and applications. In *Encyclopedia of Complexity and Systems Science*, pages 3142–3176. 2009. 2

[22] A. Seyfried, M. Boltes, J. Kähler, W. Klingsch, A. Portz, T. Rupprecht, A. Schadschneider, B. Steffen, and A. Winkens. Enhanced empirical data for the fundamental diagram and the flow through bottlenecks. In *Pedestrian and Evacuation Dynamics*, pages 145–156. Springer, 2010. 2

[23] A. Seyfried, A. Portz, and A. Schadschneider. Phase coexistence in congested states of pedestrian dynamics. ACRI, 2010. 2

[24] A. Seyfried and A. Schadschneider. Empirical results for pedestrian dynamics at bottlenecks. In *Parallel Processing and Applied Mathematics*, 2010. 2

[25] A. Seyfried, B. Steffen, W. Klingsch, and M. Boltes. The fundamental diagram of pedestrian movement revisited. *Transportation Science*, 39(1):1–24, 2005. 2, 3

[26] B. Steffen and A. Seyfried. Methods for measuring pedestrian density, flow, speed and direction with minimal scatter. *Physica A*, 389(9):1902–1910, 2010. 2

[27] U. Weidmann. Transporttechnik der Fussgänger. Technical Report 90, ETH Zürich, 1993. 2, 5